Heliyon 10 (2024) e38260

Contents lists available at ScienceDirect

Heliyon

journal homepage: www.cell.com/heliyon

Research article

Physiological and differential protein expression analyses of the calcium stress response in the *Drynaria roosii* rhizome

Yilin Wu [1], Hui Li [1], Shanshan Ma, Hongna Ma, Longyan Tan [*]

School of Pharmacy, Guizhou University of Traditional Chinese Medicine, Guiyang, 550025, China

Abbreviations: 14-3-3F, 14-3-3-like protein F; 4CL, 4-coumarate-CoA ligase; 2MF3R, 2-methylene-furan-3-one reductase; 3PS1CT2, 3-phosphoshikimate 1-carboxyvinyltransferase 2; 6PFK7, 6-phosphofructokinase 7; 26S6AB, 26S proteasome regulatory subunit 6A homolog B; 26S8A, 26S proteasome regulatory subunit 8 homolog A; 26SN6, 26S proteasome non-ATPase regulatory subunit 6 homolog; 26SN11, 26S proteasome non-ATPase regulatory subunit 11 homolog; 40S-SA, 40S ribosomal protein SA; AAO, ascorbate oxidase; ACCTβ, acetyl-coenzyme A carboxylase carboxyl transferase subunit β; ADD2, arogenate dehydratase/prephenate dehydratase 2; ADH5, alcohol dehydrogenase-like 5; AID, alkaline/neutral invertase D; API5, apoptosis inhibitor 5-like protein API5; APX, ascorbate peroxidase; ATPase3, plasma membrane ATPase 3; BAD, bifunctional aspartokinase/homoserine dehydrogenase; BP, biological processes; BSK, brassinosteroid-signaling kinase; BSK1, serine/threonine-protein kinase BSK1; BSK2, serine/threonine-protein kinase BSK2; C4H, cinnamate 4-hydroxylase; CAT2, catalase isozyme 2; CC, cellular components; CDCP48, cell division cycle protein 48 homolog; CHMP1B, ESCRT-related protein CHMP1B; CP71B10, cytochrome P450 71B10; CPI, cysteine proteinase inhibitor; CPK12, calcium-dependent protein kinase 12; CPK17, calcium-dependent protein kinase 17; CSDS, cyclin-SDS; D2A, dynamin-2A; D4DR, bifunctional dTDP-4-dehydrorhamnose 3,5-epimerase/dTDP-4-dehydrorhamnose reductase; DEP, differentially expressed protein; DHAR, dehydroascorbate reductase; DHF4R, dihydroflavonol 4-reductase; DRP1E, phragmoplastin DRP1E; E2-2, ubiquitin-conjugating enzyme E2 2; E2-7, ubiquitin-conjugating enzyme E2 7; EF2, elongation factor 2; FBA8, fructose-bisphosphate aldolase 8; FQR1-3, NAD(P)H dehydrogenase (quinone) FQR1-like 3; G3PDH, glyceraldehyde-3-phosphate dehydrogenase; GBSS1, granule-bound starch synthase 1; GDH, glutamate dehydrogenase; GlyRL, glycine–tRNA ligase, mitochondrial 1; GNDDI, guanosine nucleotide diphosphate dissociation inhibitor; GO, gene ontology; GOA, gene ontology annotation; GPX, glutathione peroxidase; GR, glutathione reductase; H2B, histone H2B; Hop1, Hsp70-Hsp90 organizing protein 1; HPD, 4-hydroxyphenylpyruvate dioxygenase; HSP17.9, 17.9 kDa class I heat shock protein; HSP70-2, heat shock 70 kDa protein 2; L3, 60S ribosomal protein L3; L9-2, 60S ribosomal protein L9-2; L10, 60S ribosomal protein L10; L13, 60S ribosomal protein L13; L15-2, 60S ribosomal protein L15-2; L21-1, 60S ribosomal protein L21-1; L21-2, 60S ribosomal protein L21-2; L23, 60S ribosomal protein L23; L23a, ribosomal protein L23a; MDA, malondialdehyde; MDHAR, monodehydroascorbate reductase; MF, molecular functions; MPK1, mitogen-activated protein kinase 1; MPKK6, mitogen-activated protein kinase kinase 6; NADPH, nicotinamide adenine dinucleotide phosphate; NDPK3, nucleoside diphosphate kinase 3; NDUIS2, NADH dehydrogenase [ubiquinone] iron-sulfur protein 2; P2D3DA1, phospho-2-dehydro-3-deoxyheptonate aldolase 1; PAL, phenylalanine ammonia-lyase; PB3, proteasome subunit beta type-3; PEPC, phosphoenolpyruvate carboxylase; PEPCK, phosphoenolpyruvate carboxykinase; PGM, phosphoglucomutase; PIP1-2, aquaporin PIP1-2; POD, peroxidase; Prx2B, peroxiredoxin-2B; RAB1BV, ras-related protein RAB1BV; RABC1, ras-related protein RABC1; RABC2a, ras-related protein RABC2a; RABD2c, ras-related protein RABD2c; RABG3b, ras-related protein RABG3b; Ran-B1, GTP-binding nuclear protein Ran-B1; RBOH, respiratory burst oxidase homolog; RBP, Ran-binding protein; RBP1c, ran-binding protein 1 homolog c; ROS, reactive oxygen species; S3-3, 40S ribosomal protein S3-3; S6, 40S ribosomal protein S6; S8, 40S ribosomal protein S8; S10-2, 40S ribosomal protein S10-2; S16, 40S ribosomal protein S16; S25-4, 40S ribosomal protein S25-4; SAMA3, s-adenosylmethionine synthase 3; SAMS2, s-adenosylmethionine synthase 2; SAPK7, serine/threonine-protein kinase SAPK7; SerRL, serine–tRNA ligase; SL13S-L1, seed linoleate 13S-lipoxygenase-1; SOD, superoxide dismutase; SOS, salt overly sensitive; SP2Aγ, serine/threonine-protein phosphatase 2A 65 kDa regulatory subunit A gamma isoform; SRK2A, serine/threonine-protein kinase SRK2A; Tα3, tubulin alpha-3 chain; Tα4, tubulin alpha-4; TIPA, TIP-like aquaporin; Trx, thioredoxin; UAD1, UDP-glucuronic acid decarboxylase 1; UAM1, UDP-arabinopyranose mutase 1; US1, UDP-D-apiose/UDP-D-xylose synthase 1; VAD1, protein VASCULAR ASSOCIATED DEATH 1; VFA, vesicle-fusing ATPase; VPAB2, v-type proton ATPase subunit B2; VPAD, v-type proton ATPase subunit D; VPAE1, v-type proton ATPase subunit E1.

* Corresponding author.
E-mail address: lytan1982@126.com (L. Tan).

[1] Co-first authors.

https://doi.org/10.1016/j.heliyon.2024.e38260
Received 28 January 2023; Received in revised form 15 September 2024; Accepted 20 September 2024
Available online 21 September 2024

ARTICLE INFO

Keywords:
Ca^{2+}
Physiology
Proteomics
Drynaria roosii rhizome
Karst

ABSTRACT

High concentration Ca^{2+} in karst soil is harmful to agriculture. Some dominant plants can adapt well to karst soil, but how Ca^{2+} affect plant is unknown. *Drynaria roosii* is a Ca^{2+}-tolerant fern and its dry rhizome is a common Chinese medicine of Miao nationality in Guizhou, China. This study analyzed the physiological and proteomic characteristics of the rhizome of *D. roosii* under calcium stress. Physiological results indicated that calcium stress may lead to osmotic stress. Proteomic results showed that 147 differentially expressed proteins (96 increased, 51decreased) were identified under calcium stress, and these proteins mainly involved in signal transduction, protein translation, material transport, antioxidant defense and secondary metabolism. This study will lay a foundation for studying the calcium adaptation mechanism of *D. roosii* at the molecular level.

1. Introduction

China's karst areas accounts for about 1/6 of the world's karst area [1,2]. Karst biotope is vulnerable, with high concentration calcium ions in their shallow soils [2]. Calcium ions participate in many biological processes of plant cells, such as signaling that induced modification of plant development, Ca^{2+} homeostasis across the plant membranes and cell wall remodeling, etc. [3–5]. High concentration Ca^{2+} affects the soil properties and the mineral elements absorption of plants [6]. Also, Ca^{2+} is extremely toxic when present at a concentration above 10^{-4} mol in the cytosol, leading to clumping of proteins and nucleic acids and disrupting the integrity of the phospholipid bilayer in the cell membrane due to the precipitation of phosphates [5]. Thus, to ensure normal physiological activity, evolution has favored the need of maintaining low cytosolic Ca^{2+} in the phosphate-rich environment of the cytosol, which would in turn grant adequate sensitivity and speed to the signals arising in the cells [5,7]. Plant cells remove excessive calcium ions by various systems, such as gated Ca^{2+} channels (e.g. hyperosmolality-gated calcium-permeable channels and cyclic nucleotide-gated channels), energy-driven pumps and exchangers that are localized in organelle membranes, the plasma membrane along with the Ca^{2+}-binding proteins localized within the cell and calcium-dependent protein kinase (e.g. CPK12, calcium-dependent protein kinase 12) [5,8,9]. Under high concentration Ca^{2+}, there is a limit to the amount of Ca^{2+} that plant cells can absorb, beyond which chloroplasts will be directly damaged, photosynthesis will be affected and blade aging was accelerated [10]. So plants adapt to karst high concentration Ca^{2+} environment by thickening cell walls, enriching calcium ions, excreting calcium ions, activating genes and enzymes induced by high concentration Ca^{2+}, and regulating the synthesis of related metabolites [11–13]. Unfortunately, previous studies on karst-specific plant species are scarce, and the adaptation mechanisms of karst-specific plant to karst environmental were rarely studied. Yet such information is important for understanding the adaptive strategies of plant species in karst area. Our findings provide a basis for discovering the adaptive mechanism of karst plants.

Proteomics technology plays an active role in analyzing plant adaptation to abiotic stress [14,15]. Understanding the regulation strategy of calcium stress at the protein level will help the breeding of new varieties in karst areas. *Drynaria roosii* is a typical plant in karst area [16]. Its dry rhizome is a common folk traditional Chinese medicine in Guizhou, China. We observed the physiological and proteomic characteristics of *D. roosii* rhizome under calcium stress. Several pathways, such as signaling, protein translation, material transport, antioxidant defense and synthesis and degradation of secondary metabolites were affected by calcium stress. The results are helpful to understand the mechanism of adaptation of *D. roosii* to karst habitat.

2. Materials and methods

The experimental conditions with respect to plant materials, growth conditions and stress treatments were similar to those in Wu et al. [17] barring the light condition which was adjusted to 50 μmol m^{-2} s^{-1}. The water content, MDA content, soluble sugar content and enzyme activity were carried out as per Wu et al. [17].

The proteins were extracted as described previously [18]. The protein digestion was primarily performed as per the Filter Aided Sample Preparation (FASP) protocol [19]. Each sample was separated by a high-performance liquid phase system, EASY-nLC with a nanoliter flow rate. The chromatographic column was balanced with 95 % buffer A (0.1 % formic acid aqueous solution). The sample was loaded onto the loading column (Thermo Scientific Acclaim PepMap 100, 100 μm × 2 cm, Nanoviper C18) by an automatic sampler and then separated by an analysis column (Thermo Scientific EASY-Column, 10 cm, ID75 μm, 3 μm, C18-A2) at a flow rate of 300 nL·min^{-1} by IntelliFlow technology. Samples were separated by liquid chromatography and analyzed by a Q Exactive mass spectrometer. The analysis duration was 60/120/240 min, the positive ion mode was used for detection, the scanning range of the parent ions was 300–1800 *m/z*, the primary mass spectrum resolution was 70,000 at 200 *m/z*, the AGC target was 3e6, the primary maximum IT was 10 ms, the number of scan ranges was 1, and the dynamic exclusion was 40 s. The mass-to-charge ratio of polypeptides and polypeptide fragments was determined according to the following methods: 10 fragment patterns (MS2 scan) were collected after each full scan, the MS2 activation type was HCD, the isolation window was 2 *m/z*, the secondary mass spectrum resolution was 17,500 at 200 *m/z*, there was 1 microscan, the secondary maximum was 60 ms, the normalized collision energy was 30 eV, and the underfill was 0.1 %. The nine resulting raw LC-MS/MS files were imported to the Maxquant software (1.6.14) for database inquiry and LFQ label-free quantification analysis. The database was uniprot_hbk_20220411.fasta. The database search and differentially expressed proteins (DEPs) selection were the same as those of Wu et al. [17]. The CELLO (http://cello.life.nctu.edu.tw/) method was used for the predicating subcellular localization of DEPs. The InterProScan (interproscan-5.25-64.0) was used for

predicating domain of DEPs. The Gene Ontology (GO) annotations of the DEPs were derived from the UniProtKB (http://www.uniprot.org/help/uniprotkb/) at the Gene Ontology Annotation (GOA) (http://www.ebiac.uk/GOA/) database. Function analysis of DEPs was performed with Blast2Go (BLASTP 2.8.0+) using GO functional annotation, and proteins were categorized according to their biological process, molecular function, and cellular localization. According to the function of the DEPs, the possible metabolic pathways involved in these DEPs were classified.

Statistical analysis was the same as that of Wu et al. [17], and a p-value less than 0.05 was considered statistically significant.

3. Results

3.1. Physiological changes by excessive calcium ions treatment

Water content was decreased 5.14 % and 13.49 % by 600 and 1200 mmol L^{-1} Ca^{2+}, respectively (Fig. 1A). Soluble sugar content increased 22.79 % and 50.03 %, respectively (Fig. 1B). Meanwhile, MDA content increased 8.82 % and 24.2 %, respectively (Fig. 1C). Activity of superoxide dismutase (SOD), peroxidase (POD) and catalase (CAT) increased by excessive calcium ions treatment also; the biggest difference was that SOD increased significantly by 600 mmol L^{-1} Ca^{2+}, while POD and CAT increased less. (Fig. 1D–F).

3.2. Proteins changes by excessive calcium ions treatment

We identified 743 proteins, among these proteins, 7 proteins are unique to R-0 sample (0 mmol L^{-1} Ca^{2+} treated rhizome), 13 proteins are unique to R-600 sample (600 mmol L^{-1} Ca^{2+} treated rhizome), 2 proteins are unique to R-1200 sample (1200 mmol L^{-1} Ca^{2+} treated rhizome); 692 proteins are common to R-0 sample and R-600 sample, 702 proteins are common to R-600 sample and R-1200 sample, 683 proteins are common to R-0 sample and R-1200 sample; and 678 proteins are common to R-0 group, R-600 group and R-1200 group (Fig. 2).

There are 63 DEPs (47 increased, 16 decreased) in R-600_vs_R-0 group; 44 DEPs (33 increased, 11 decreased) in R-1200_vs_R-0 group; 40 DEPs (16 increased, 24 decreased) in R-1200_vs_R-600 group (Fig. 3A–C, 4A-B). For the up-regulated DEPs in the three groups, 39 DEPs are unique to R-600_vs_R-0 group; 24 proteins are unique to R-1200_vs_R-0 group; 15 proteins are unique to R-1200_vs_R-600 group; 8 DEPs are common to R-600_vs_R-0 group and R-1200_vs_R-0 group; 1 DEP is common to R-1200_vs_R-0 group and R-1200_vs_R-600 group; there is no protein common to R-600_vs_R-0 group and R-1200_vs_R-600 group or the three groups (Fig. 4A). For the down-regulated proteins in the three groups, there are 14 proteins were unique to R-600_vs_R-0 group; 9 proteins were unique to R-1200_vs_R-0 group; 24 proteins were unique to R-1200_vs_R-600 group; 2 DEPs are common to R-600_vs_R-0 group and R-1200_vs_R-0 group; there is no protein common to R-1200_vs_R-0 group and R-1200_vs_R-600 group, R-600_vs_R-0 group and R-1200_vs_R-600 group or the three groups (Fig. 4B).

Screened differential proteins were divided into biological processes (BP), molecular functions (MF), and cellular components (CC). In R-600_vs_R-0 group, the most significant GO terms mainly include protein modification, transferase, and membrane related (Fig. 5A). In R-1200_vs_R-0 group, the most significant GO terms mainly include macromolecule biosynthesis and organelle related (Fig. 5B). In R-1200_vs_R-600 group, the most significant GO terms mainly include peptide, ribosome, organelle, ribonucleoprotein, and vacuole. (Fig. 5C).

According to the function of the differentially expressed proteins, the possible metabolic pathways involved in these differentially expressed proteins were classified (Tables 1–6, Supplementary Tables 1–3). In R-600_vs_R-0 group, there are 8 DEPs (8 increased, including MPK1, MPKK6, 14-3-3F, ATPase3, BSK1, BSK2, SP2Aγ, and CPK17) participate in Signal transduction; 13DEPs (12 increased, including GlyRL, L3, L21–1, L10, S25–4, S10–2, S3-3, 26S8A, 26SN6, 26SN11, E2-2 and E2-7; 1 decreased, HSP17.9) participate in Protein metabolism; 2DEPs (2 increased, including SL13S-L1 and ACCTβ) participate in Lipid metabolism; 6DEPs (2 increased, including PEPC and AID; 4 decreased, including G3PDH, FBA8, NDUIS2 and GBSS1) participate in Carbohydrate and energy metabolism; 7DEPs (5 increased, including RBP1c, VPAB2, VFA, D2A and TIPA; 2 decreased, including GNDDI and VPAD) participate in Material Transport; 6DEPs (3 increased, including US1, UAD1 and actin 3; 3 decreased, including actin, actin-1 and actin-2) participate in Cell wall and cytoskeleton; 2 DEPs (2 increased, including CSDS and DRP1E) participate in Cell division; 4 DEPs (3 increased, including CAT2, chitinase A and CP71B10; 1 decreased, FQR1-3) participate in Antioxidant and defense; 8DEPs (7 increased, including P2D3DA1, 3PS1CT2, SAMA3, ADD2, 2C4H and a DHF4R; 1 decreased, 2MF3R) involved in Secondary metabolism (Tables 1 and 2, Supplementary Table 1). In R-1200_vs_R-0 group, there are 3 DEPs (3 increased, including SAPK7, SP2Aγ and calmodulin 1) participate in Signal transduction; 11DEPs (10 increased, including EF2, SerRL, L23, L9-2, 40S-SA, S3-3, Hop1, prohibitin-5, 26S8A and 26S6AB; 1 decreased, L15-2) participate in Protein metabolism; 1DEP (1 decreased, GDH) participate in Amino acid metabolism; 5DEPs (2 increased, including transketolase and PEPCK; 3 decreased, including PGM, NDUIS2 and NDPK3) participate in Carbohydrate and energy metabolism; 8DEPs (7 increased, including Ran-B1, RAB1BV, RABG3b, RABD2c, dynamin-2A, CHMP1B and VPAB2; 1 decreased, PIP1-2) participate in Material Transport; 2DEPs (1 increased, UAM1; 1 decreased, Tα3) participate in Cell wall and cytoskeleton; 1 DEP (1 increased, CDCP48) participate in Cell division; 3 DEPs (3 increased, Prx2B, chitinase A and VAD1) participate in Antioxidant and defense; 6DEPs (5 increased, including 3PS1CT2, 3 PAL and a C4H; 1 decreased, 2MF3R) participate in Secondary metabolism (Tables 3 and 4, Supplementary Table 2). In R-1200_vs_R-600 group, there are 1 DEP (1 decreased, SRK2A) participate in Signal transduction; 1 DEP (1 decreased, H2B) participate in Nucleic acid metabolism; 12DEPs (2 increased, including PB3 and ubiquitin; 10 decreased, including GlyRL, L13, L21–2, L10, S6, S8, S16, S25–4, L23a and HSP70-2) participate in Protein metabolism; 1DEP (1 increased, BAD) participate in Amino acid metabolism; 3DEPs (1 increased, G3PDH; 2 decreased, 6PFK7 and ADH5) participate in Carbohydrate and energy metabolism; 8DEPs (6 increased, RABG3b, RABC1, RABC2a,

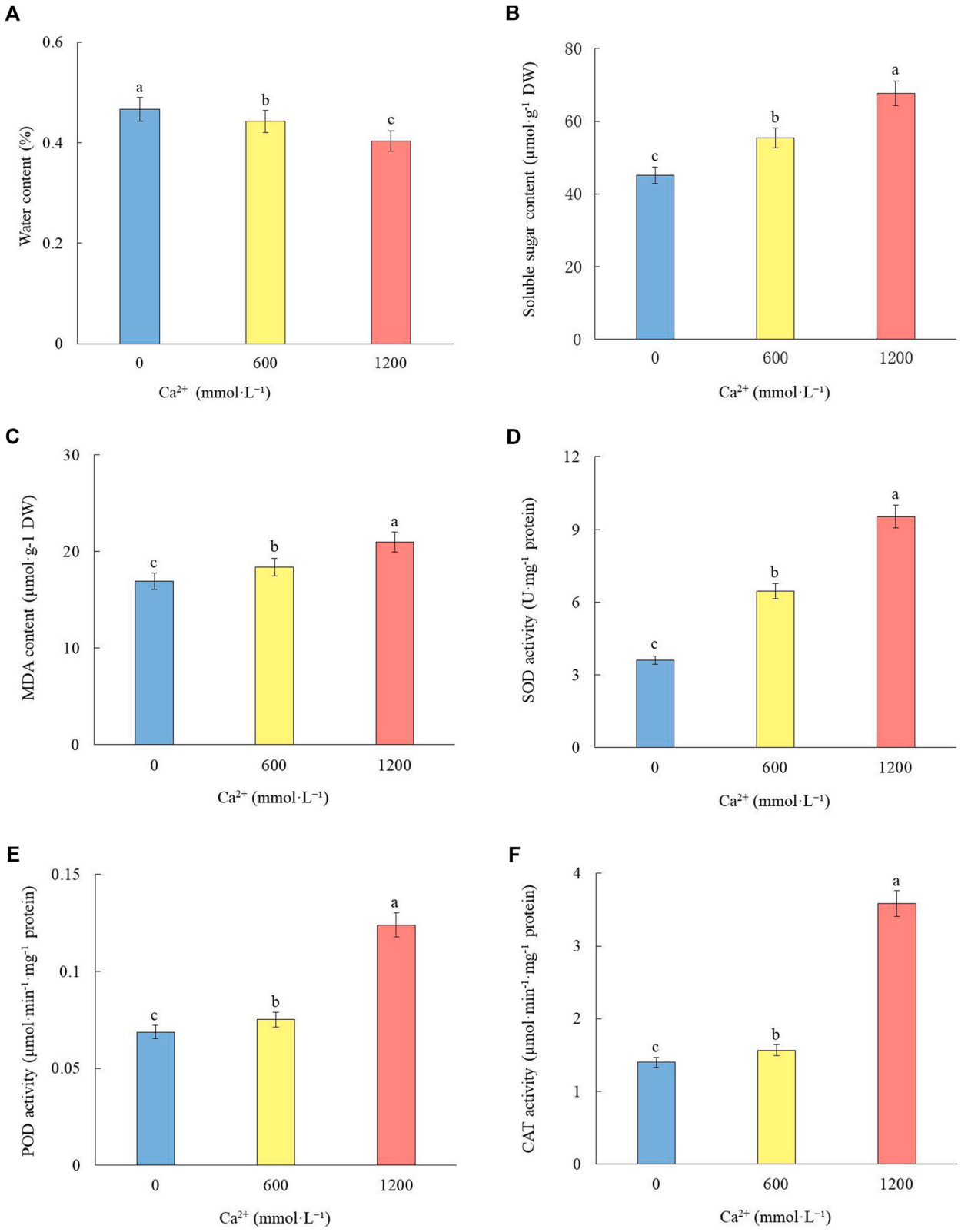

(caption on next page)

Fig. 1. Effects of Ca^{2+} stress on water content, osmotic homeostasis, membrane integrity, activities of antioxidant enzymes in *D. roosii* rhizome. (A) Water content; (B) Soluble sugar content; (C) MDA content; (D) SOD activity; (E) POD activity; (F) CAT activity. The values were determined after plants were treated with 0, 600, and 1200 mmol·L-1 Ca^{2+} for 14 days, and were presented as means ± SE (n = 6). The small letters indicate significant difference ($p < 0.05$).

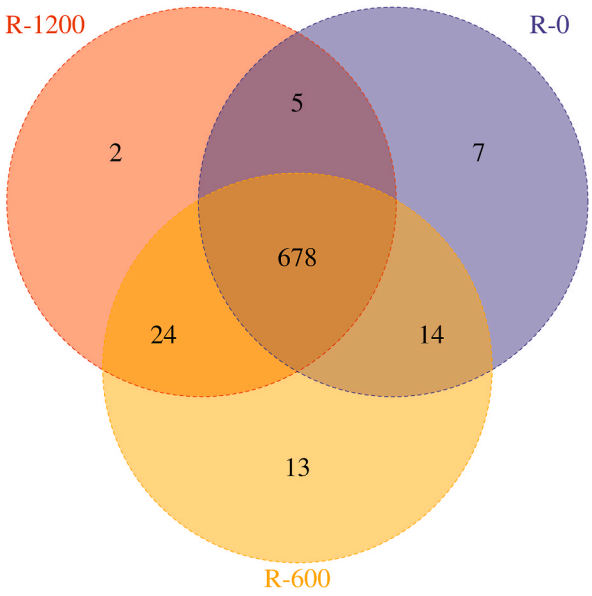

Fig. 2. Venn diagram of identified proteins of different treatments in *D. roosii* rhizome.

GNDDI, VPAE1 and VPAD; 2 decreased, including ATPase 3 and TIPA) participate in Material Transport; 1DEP (1 decreased, Tα4) participate in Cell wall and cytoskeleton; 3 DEPs (2 increased, including CPI and HPD; 1 decreased, API5) participate in Antioxidant and defense; 5DEPs (5 decreased, including SAMS2, SAMS3, P2D3DA1, D4DR and REF1) participate in Secondary metabolism (Tables 5 and 6, Supplementary Table 3).

4. Discussion

4.1. Calcium stress may cause osmotic stress and oxidative damage of D. roosii rhizome

Calcium stress may damages cells by producing reactive oxygen species (ROS) through osmotic stress and eventually leads to inhibition of plant growth [20–22]. Soluble sugar can be used as osmotic protective substance [20–22]. In the present research, the water content decreased by calcium stress, but the soluble sugar content increased (Fig. 1A and B), suggesting that soluble sugar may play a role in regulating osmotic pressure. MDA production indicates membrane peroxidation [23,24]. Calcium stress can cause MDA production, which has been confirmed in other studies [20–22]. The same results were obtained in this study (Fig. 1C), suggesting oxidative damage to the membrane. In plants, the increase of antioxidant enzyme activity can effectively eliminate the ROS produced by stress [25]. In the present research, the increase of the activity of three antioxidant enzymes may indicate that they play an important role in scavenging ROS (Fig. 1D–F). However, when plants were subjected to heavy metal, salt and osmotic stress, appropriate increase of exogenous calcium ions may alleviate stress toxicity. For example, *TaNCL2-A* (a sodium/calcium exchanger-like transporter) expressing transgenic *Arabidopsis* lines exhibited significant Cd tolerance with increased Ca (~10 fold) accumulation [26]. Meanwhile, the transgenic lines exhibited significant salinity and osmotic stress tolerance, suggesting that the *TaNCL2-A* could mitigate Cd toxicity along with salinity and osmotic stress [26]. These results showed the regulatory role of calcium ions when they were not used as a stress factor.

4.2. Calcium stress may affect signal transduction of D. roosii rhizome cells

MPK cascades play important roles in plants response to stresses [27]. Study had shown that the transcription of *ATMPK1* was promoted by salt stress [28]. Meanwhile, overexpression of MPKK6 in rice showed good salt stress tolerance [29]. In this study, we found MPK1 and MPKK6 was increased by 600 mmol L^{-1} Ca^{2+}, indicating that MPK1 and MPKK6 mediated signal transduction pathways may be enhanced by calcium stress in *D.roosii* rhizome cells. 14-3-3 proteins can also participate in the signal pathways of plant response to environment [30]. CDPKs could convert intracellular calcium signals into reversible phosphorylation of various substrates, and which interact with 14-3-3 proteins to further regulate the function of proteins to adapt to stress environment [31]. For

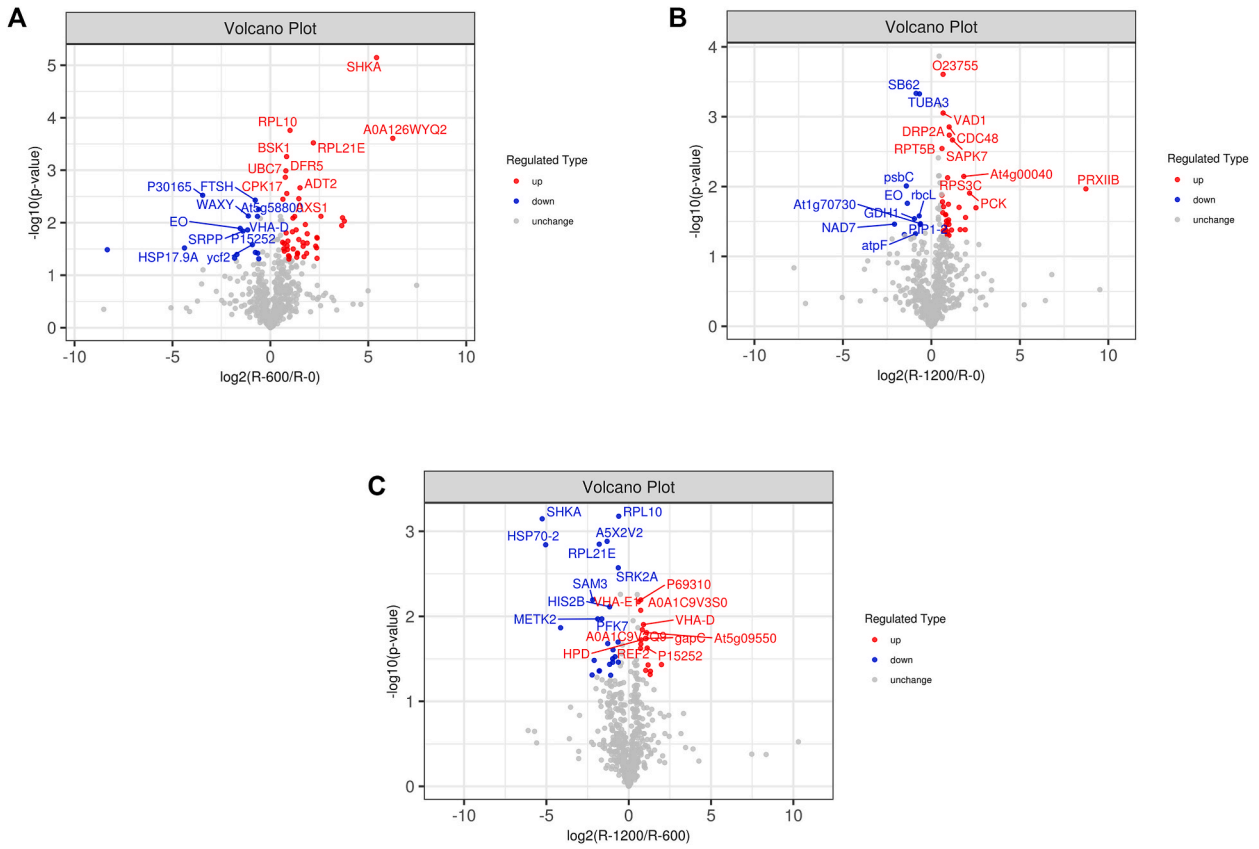

Fig. 3. Volcano plots of identified proteins of different comparison groups in *D. roosii* rhizome. (A) R-600_vs_R-0 group; R-1200_vs_R-0 group; R-1200_vs_R-600 group. In the plots, the red dots are the significantly up-regulated differentially expressed proteins (DEPs), the blue dots are the significantly down-regulated DEPs, and the gray dots are the proteins with no difference changes.

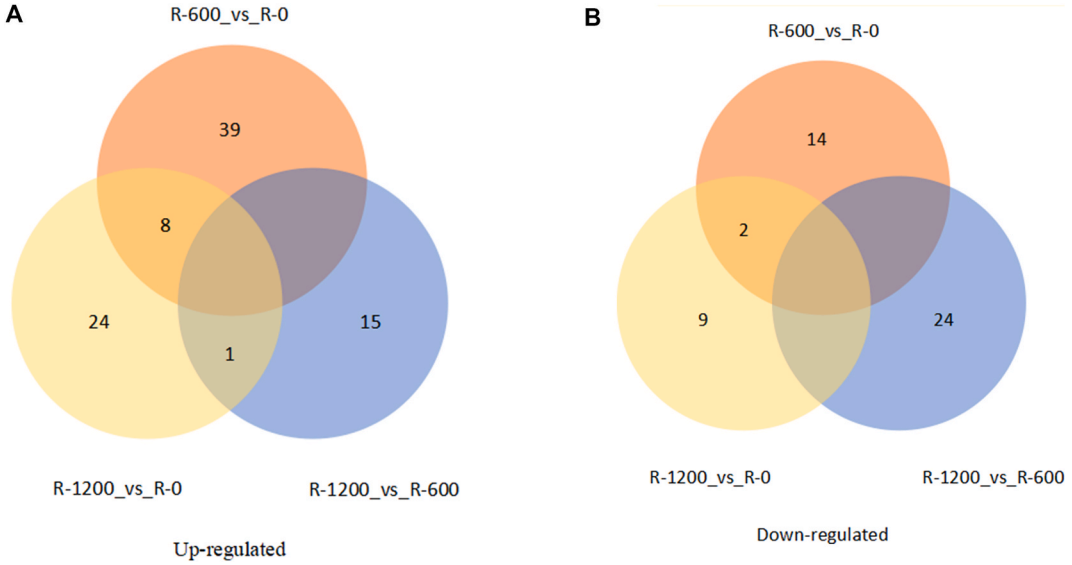

Fig. 4. Venn diagrams of DEPs between different comparison groups in *D. roosii* rhizome. (A) Up-regulated DEPs of R-600_vs_R-0 group, R-1200_vs_R-0 group and R-1200_vs_R-600 group; (B) Down-regulated DEPs of R-600_vs_R-0 group, R-1200_vs_R-0 group and R-1200_vs_R-600 group.

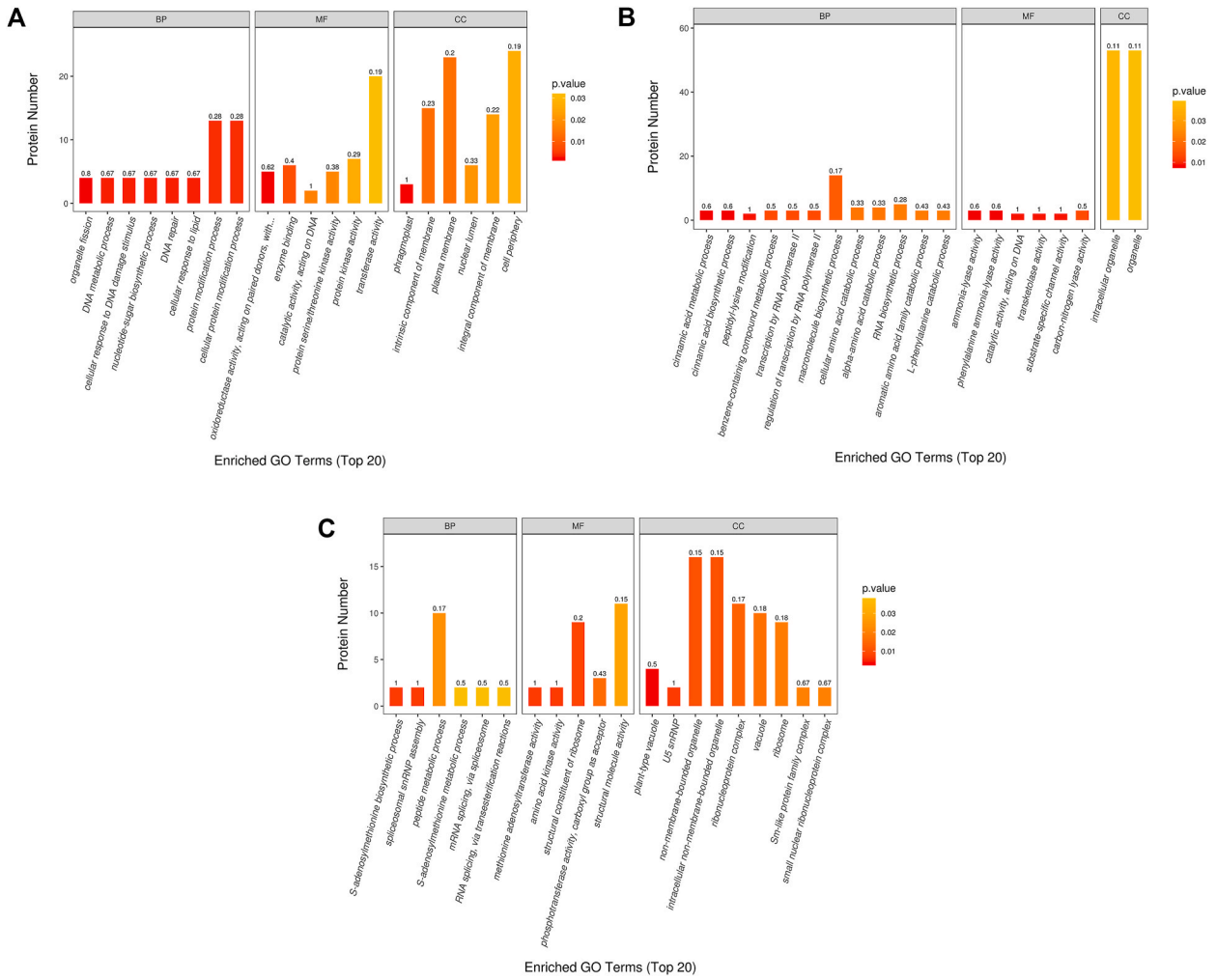

Fig. 5. Top 20 GO terms of the DEPs of different comparison groups in *D. roosii* rhizome. (A) R-600_vs_R-0 group; R-1200_vs_R-0 group; R-1200_vs_R-600 group.

example, OsCDPK1 can activate 14-3-3 protein in rice seedlings to enhance the tolerance to drought stress [32]. 14-3-3 proteins can also interact with H^+- ATPase to regulate ion channels to adapt to abiotic stress. Guo et al. [33] reported that Al stress could induce the interaction of H^+-ATPase and 14-3-3 protein in black soybean. In addition, 14-3-3 proteins may enhance stress tolerance by participating in hormone signaling pathways, such as ABA signaling pathway [34]. Meanwhile, calmodulin 1 participates in the Ca^{2+} signaling pathway promotes the production of ROS [35].The results in this research indicated that, 14-3-3 F, CPK17, and ATPase3 were increased by 600 mmol L^{-1} Ca^{2+}, and calmodulin 1 was increased by 1200 mmol L^{-1} Ca^{2+} also (Tables 1 and 3). The plant BSK and phosphatase 2A play important roles in brassinosteroid responsive signal transduction [36,37]. And, SAPK7 was activated in response to osmotic stress [38]. Our results also indicated that BSK1 and BSK2 were increased by 600 mmol L^{-1} Ca^{2+}; and SAPK7 was increased by 1200 mmol L^{-1} Ca^{2+}; SP2Aγ was increased by the both treatments (Tables 1 and 3). Thus, the signal transduction pathways involved in these signal molecules in *D. roosii* rhizome cells may be affected by calcium stress. Excessive ROS cause oxidative damage to plants, but a limited level of ROS play an essential role in signaling during stress response. It has been reported that the respiratory burst oxidase homologs (RBOH) enzymes are plant-specific NADPH oxidases responsible for the generation of ROS within the apoplast [39]. And the protein-protein interactions predicted the interaction of bread wheat RBOHs proteins with many proteins involved in ROS mediated stress response, including calcineurin B-like interacting protein kinases, calcineurin B-like calcium sensor proteins, calcium dependent protein kinases, mitogen-activated protein kinase 3, etc. [40]. Thus, these signal transduction mechanisms involved in calcium stress still need to be further studied.

4.3. Calcium stress may regulate protein translation in D. roosii rhizome cells

Ribosomes, function in protein synthesis, consist of two subunits [41]. In our proteomics results, a GlyRL, six ribosomal subunits were increased by 600 mmol L^{-1} Ca^{2+}; an EF2, a SerRL, four ribosomal subunits were increased by 1200 mmol L^{-1} Ca^{2+} (Tables 1 and

Table 1
Up-regulated DEPs of R-600_vs_R-0 group.

Accession number	Protein Name	Gene Name	R-600/R-0 (FC)	*p* value
Signal transduction (8)			76.121	0.000
Q08436	Plasma membrane ATPase 3	PMA3	2.733	0.021
Q84UI5	Mitogen-activated protein kinase 1	MPK1	3.669	0.025
Q9FJV0	Mitogen-activated protein kinase kinase 6	MKK6	1.858	0.022
O49998	14-3-3-like protein F		1.927	0.049
Q9LS26	Serine/threonine-protein kinase BSK2	BSK2	1.776	0.001
Q944A7	Serine/threonine-protein kinase BSK1	BSK1	1.810	0.028
Q38951	Serine/threonine-protein phosphatase 2A 65 kDa regulatory subunit A gamma isoform	PP2AA3	1.789	0.003
Q9FMP5	Calcium-dependent protein kinase 17	CPK17	76.121	0.000
Protein metabolism (12)				
O23627	Glycine–tRNA ligase, mitochondrial 1	At1g29880	5.981	0.008
P35684	60S ribosomal protein L3	RPL3	5.207	0.048
Q9FDZ9	60S ribosomal protein L21-2	RPL21E	4.568	0.000
P45633	60S ribosomal protein L10	RPL10	2.004	0.000
Q9T029	40S ribosomal protein S25-4	RPS25E	2.537	0.046
Q9FFS8	40S ribosomal protein S10-2	RPS10B	1.903	0.043
Q9FJA6	40S ribosomal protein S3-3	RPS3C	1.637	0.035
Q9C5U3	26S proteasome regulatory subunit 8 homolog A	RPT6A	3.444	0.011
Q93Y35	26S proteasome non-ATPase regulatory subunit 6 homolog	RPN7	1.830	0.032
Q9LP45	26S proteasome non-ATPase regulatory subunit 11 homolog	RPN6	1.557	0.004
P25866	Ubiquitin-conjugating enzyme E2 2	UBC2	2.490	0.014
P25868	Ubiquitin-conjugating enzyme E2 7	UBC7	1.697	0.001
Lipid metabolism (2)				
P08170	Seed linoleate 13S-lipoxygenase-1	LOX1.1	12.481	0.011
A0A5B9RDW7	Acetyl-coenzyme A carboxylase carboxyl transferase subunit beta	accD	3.680	0.016
Carbohydrate and energy metabolism (2)				
Q8VXK2	Phosphoenolpyruvate carboxylase (Fragment)	ppc	1.631	0.025
F4I2X9	Alkaline/neutral invertase D	INVD	3.606	0.038
Material Transport (5)				
P92985	Ran-binding protein 1 homolog c	RANBP1C	12.837	0.008
Q9SZN1	V-type proton ATPase subunit B2	VHA-B2	1.544	0.024
Q9M0Y8	Vesicle-fusing ATPase	NSF	3.281	0.044
Q9SE83	Dynamin-2A	DRP2A	3.164	0.024
M9YX97	TIP-like aquaporin	AQP1	13.674	0.009
Cell wall and cytoskeleton (3)				
Q9ZUY6	UDP-D-apiose/UDP-D-xylose synthase 1	AXS1	2.734	0.003
Q8VZC0	UDP-glucuronic acid decarboxylase 1	UXS1	5.230	0.020
O82565	Actin 3		5.132	0.030
Cell division (2)				
Q1PFW3	Cyclin-SDS	SDS	1.953	0.045
Q9FNX5	Phragmoplastin DRP1E	DRP1E	2.356	0.008
Antioxidant defense (3)				
P55308	Catalase isozyme 2	CAT2	2.243	0.032
Q0WYK2	Chitinase A	prchiA	5.181	0.019
Q9LVD2	Cytochrome P450 71B10	CYP71B10	1.747	0.016
Secondary metabolism (7)				
P21357	Phospho-2-dehydro-3-deoxyheptonate aldolase 1	SHKA	42.900	0.000
P23281	3-phosphoshikimate 1-carboxyvinyltransferase 2	EPSPS-2	2.601	0.039
Q9SSE7	Arogenate dehydratase/prephenate dehydratase 2	ADT2	2.848	0.002
W5XMH0	Cinnamate 4-hydroxylase	C4H	2.225	0.008
B9VV87	Cinnamate 4-hydroxylase (Fragment)		1.608	0.032
A0A5P8I1Z5	Dihydroflavonol 4-reductase	DFR5	1.730	0.001
P50303	S-adenosylmethionine synthase 3	SAM3	3.191	0.028
Other (3)				
A0A126WYQ2	LOV domain-containing protein		2.606	0.038
Q9XF89	Chlorophyll *a-b* binding protein CP26, chloroplastic	LHCB5	4.969	0.028
A0A0B5EH65	Photosystem I P700 chlorophyll a apoprotein A1	psaA	2.183	0.015

3). Meanwhile, our proteomics results also revealed that a hop1 and a prohibitin-5 were increased by 1200 mmol L^{-1} Ca^{2+} (Table 3). Hsp70 and Hsp90 play a role in the early folding and stability of protein, respectively [42]. The hop1 could regulate the activities of Hsp70 and Hsp90 [42]. Prohibitin has a role in stabilizing unassembled membrane proteins [43]. These results suggest that protein translation and folding in *D. roosii* rhizome cells may be regulated by calcium stress. In addition, we found that three 26S proteasome proteins and two E2 proteins were increased by 600 mmol L^{-1} Ca^{2+}; and two 26S proteasome proteins were increased by 1200 mmol L^{-1} Ca^{2+} (Tables 1 and 3). This suggests that protein degradation in *D. roosii* rhizome cells may also be affected by calcium stress.

Table 2
Down-regulated DEPs of R −600_vs_ R −0 group.

Accession number	Protein Name	Gene Name	R-600/R-0 (FC)	*p* value
Protein metabolism (1)				
Q84Q77	17.9 kDa class I heat shock protein	HSP17.9A	0.048	0.030
Carbohydrate and energy metabolism (4)				
A0A5P8I1W2	Glyceraldehyde-3-phosphate dehydrogenase	GAPDH	0.589	0.037
Q9LF98	Fructose-bisphosphate aldolase 8, cytosolic	FBA8	0.307	0.040
P93306	NADH dehydrogenase [ubiquinone] iron-sulfur protein 2	NAD7	0.283	0.047
Q43784	Granule-bound starch synthase 1	WAXY	0.459	0.007
Material Transport (2)				
Q9LXC0	Guanosine nucleotide diphosphate dissociation inhibitor	At5g09550	0.663	0.049
Q9XGM1	V-type proton ATPase subunit D	VHA-D	0.634	0.008
Cell wall and cytoskeleton (3)				
P53498	Actin		0.640	0.038
P53504	Actin-1	AC1	0.003	0.033
P30165	Actin-2		0.091	0.003
Antioxidant defense (1)				
Q9LUX9	NAD(P)H dehydrogenase (quinone) FQR1-like 3	At5g58800	0.659	0.006
Secondary metabolism (1)				
K4BW79	2-methylene-furan-3-one reductase	EO	0.344	0.013
Other (4)				
Q39444	ATP-dependent zinc metalloprotease FTSH	FTSH	0.586	0.004
A0A248RFH5	Conserved hypothetical chloroplast protein ycf2	ycf2	0.529	0.026
P15252	Rubber elongation factor protein		0.448	0.014
O82803	Small rubber particle protein	SRPP	0.379	0.015

4.4. Calcium stress may regulate material transport in D. roosii rhizome cells

RBP play a role in the transport between nucleus and cytoplasm [44]. Our proteomics results suggested that, an RBP1c was increased by 600 mmol L^{-1} Ca^{2+}, and a Ran-B1 was increased by 1200 mmol L^{-1} Ca^{2+}, respectively (Tables 1 and 3). Meanwhile, we also found that a VAB2 was increased by the both treatments (Tables 1 and 3). Ran-B1 functions in nuclear transportation, modulating cell cycle, and also the ionic homeostasis of phosphorus deficient plants [45]. VPAB2 directly interact with SOS2 and function in sodium ion homeostasis [46]. And the SOS pathway plays an important role in ion transport of plant under salt stress [43]. These results suggested that nuclear transport in *D. roosii* rhizome cells may be affected by Ca^{2+} stress, and may be function in ionic homeostasis. In this research, several proteins participate in vesicle trafficking were increased, including D2A and VFA by 600 mmol L^{-1} Ca^{2+}, D2A, CHMP1B, RAB1BV, RABG3b, RABD2c by 1200 mmol L^{-1} Ca^{2+} (Tables 1 and 3). Dynamin plays a role in the formation of endocytic vesicles [47]. VFA functions in the fusion between transport vesicles and target membrane. CHMP1B plays important roles in endocytosis vesicles' sorting process and auxin carriers are cargo proteins [48]. Rab1b functions in the regulation of vesicular transport between ER and Golgi complex, and regulates the formation of autophagosome [49,50]. RabG3b has a role in autophagy [51,52]. RABD2c localize to the trans-Golgi and functions in the vesicular transport of ER to Golgi complex [53]. Also RABD2c plays important roles in mitochondrial autophagy of *Euphorbia kansui* laticifers [54]. These results suggested exocytosis, endocytosis, intracellular vesicle transport, and autophagy may be affected by calcium stress in *D. roosii* rhizome cells. In addition, a TIPA was increased by 600 mmol L^{-1} Ca^{2+}, and a PIP1-2 was decreased by 1200 mmol L^{-1} Ca^{2+} (Tables 1 and 4). High levels of aquaporins present in the tonoplast of tobacco and maize cells indicate that they play pivotal roles in cell osmoregulation [55,56] and TIPA plays a role in stomatal movements [57]. PIP1 and PIP2 aquaporins function in CO_2 transport through biological membranes [58,59]. Thus, calcium stress may also affect the transport of osmoregulatory substances and carbon dioxide in *D. roosii* rhizome cells.

4.5. Antioxidant defense may be activated by calcium stress in D.roosii rhizome cells

Stresses often perturb the homeostasis and ion distribution in plant cells and leading to ROS accumulation, SOD, POD, CAT, ascorbate peroxidase (APX), monodehydroascorbate reductase (MDHAR), dehydroascorbate reductase (DHAR), glutathione reductase (GR) and ascorbate oxidase (AAO) function in scavenging ROS [23,60–62]. Research has shown that the activity of SOD, POD, CAT, APX, MDHAR, DHAR, glutathione peroxidase (GPX) and GR in seedlings of *Puccinellia tenuiflora* was increased by 150 mmol L^{-1} $NaHCO_3$ treatment [23]. And our previous research suggested that the activity of SOD, POD and CAT, the expression abundance of SOD2, CAT3, peroxiredoxin (Prx), thioredoxin (Trx), APX and MDHAR were increased by calcium stress in *D. roosii* leaf cells [17]. In this research, the proteomic results showed that CAT2 was increased by 600 mmol L^{-1} Ca^{2+}; and Prx2B was increased by 1200 mmol L^{-1} Ca^{2+} (Tables 1 and 3). Prx2B also has role in scavenging ROS in plants [63]. CP71B10 was increased by 600 mmol L^{-1} Ca^{2+} and VAD1 was increased by 1200 mmol L^{-1} Ca^{2+}, respectively; and chitinase A was increased by the both treatments (Tables 1 and 3). Apart from defense against pathogen stress, chitinases are also induced by osmotic, salt, drought and heavy metal stresses [64,65], so chitinase A may play a role in defense under Ca^{2+} stress. Cytochrome P450s (CYPs) have a role in detoxification under stresses [66]. And VAD1 might participate in the control of vascular bundle cell apoptosis [67]. Thus, various defense mechanisms may be activated by calcium stress in *D.roosii* rhizome cells.

Table 3
Up-regulated DEPs of R-1200_vs_R-0 group.

Accession number	Protein Name	Gene Name	R-1200/R-0 (FC)	*p* value
Signal transduction (3)				
Q7XQP4	Serine/threonine-protein kinase SAPK7	SAPK7	2.286	0.002
Q38951	Serine/threonine-protein phosphatase 2A 65 kDa regulatory subunit A gamma isoform	PP2AA3	1.754	0.025
Q8LRL0	Calmodulin 1		1.928	0.032
Protein metabolism (10)				
O23755	Elongation factor 2		1.583	0.000
Q39230	Serine–tRNA ligase, cytoplasmic	At5g27470	1.759	0.042
Q9ZSR8	40S ribosomal protein SA	LRP	3.087	0.041
Q9SZX9	60S ribosomal protein L9-2	RPL9D	2.960	0.020
Q9FJA6	40S ribosomal protein S3-3	RPS3C	1.889	0.007
Q9XEK8	60S ribosomal protein L23	RPL23	1.869	0.049
Q43468	Hsp70-Hsp90 organizing protein 1	HOP1	1.561	0.024
Q9LY99	Prohibitin-5	PHB5	1.609	0.019
Q9C5U3	26S proteasome regulatory subunit 8 homolog A	RPT6A	3.758	0.042
O04019	26S proteasome regulatory subunit 6A homolog B	RPT5B	1.515	0.003
Carbohydrate and energy metabolism (2)				
O20250	Transketolase		1.593	0.043
P42066	Phosphoenolpyruvate carboxykinase (ATP)	PCK	4.467	0.012
Material Transport (7)				
P41919	GTP-binding nuclear protein Ran-B1	RAN-B1	1.961	0.030
Q39433	Ras-related protein RAB1BV	RAB1BV	1.742	0.025
O04157	Ras-related protein RABG3b	RABG3B	2.204	0.042
Q9SEH3	Ras-related protein RABD2c	RABD2C	1.513	0.013
Q9SE83	Dynamin-2A	DRP2A	2.019	0.002
Q9SSM4	ESCRT-related protein CHMP1B	CHMP1B	1.547	0.017
Q9SZN1	V-type proton ATPase subunit B2	VHA-B2	1.948	0.018
Cell wall and cytoskeleton (1)				
O04300	UDP-arabinopyranose mutase 1	UPTG	1.992	0.050
Cell division (1)				
P54774	Cell division cycle protein 48 homolog	CDC48	2.008	0.001
Antioxidant defense (3)				
Q9XEX2	Peroxiredoxin-2B	PRXIIB	424.869	0.011
Q0WYK2	Chitinase A	prchiA	5.722	0.020
F4HVW5	Protein VASCULAR ASSOCIATED DEATH 1	VAD1	1.584	0.001
Secondary metabolism (5)				
P23281	3-phosphoshikimate 1-carboxyvinyltransferase 2 (Fragment)	EPSPS-2	1.988	0.035
Q5EP59	Phenylalanine ammonia-lyase	PAL	3.812	0.028
Q5EP63	Phenylalanine ammonia-lyase	PAL	1.894	0.045
Q5EP60	Phenylalanine ammonia-lyase (Fragment)	PAL	1.810	0.031
B9VV87	Cinnamate 4-hydroxylase (Fragment)	C4H	1.777	0.035
Other (1)				
O81305	Type III polyketide synthase C	At4g00040	3.557	0.007

Table 4
Down-regulated DEPs of R-1200_vs_R-0 group.

Accession number	Protein Name	Gene Name	R-1200/R-0 (FC)	*p* value
Protein metabolism (1)				
O65082	60S ribosomal protein L15-2	SB62	0.549	0.000
Amino acid metabolism (1)				
P93541	Glutamate dehydrogenase	GDH1	0.513	0.029
Carbohydrate and energy metabolism (3)				
Q9SGC1	Phosphoglucomutase, cytoplasmic 2	At1g70730	0.651	0.034
P93306	NADH dehydrogenase [ubiquinone] iron-sulfur protein 2	NAD7	0.235	0.035
P81766	Nucleoside diphosphate kinase 3		0.346	0.049
Material Transport (1)				
Q7XSQ9	Aquaporin PIP1-2	PIP1-2	0.644	0.035
Cell wall and cytoskeleton (1)				
Q56WH1	Tubulin alpha-3 chain	TUBA3	0.627	0.000
Secondary metabolism (1)				
K4BW79	2-methylene-furan-3-one reductase	EO	0.389	0.017
Other (3)				
A0A2L0HIN0	Ribulose bisphosphate carboxylase large chain (Fragment)	rbcL	0.620	0.026
A0A219T2W6	ATP synthase CF0 B subunit (Fragment)	atpF	0.536	0.047
A0A248RBK6	Photosystem II CP43 reaction center protein	psbC	0.374	0.010

Table 5
Up-regulated DEPs of R-1200_vs_R-600 group.

Accession number	Protein Name	Gene Name	R-1200/R-600 (FC)	*p* value
Protein metabolism (2)				
Q9LST7	Proteasome subunit beta type-3	PBC1	1.644	0.024
P69310	Ubiquitin		1.661	0.006
Amino acid metabolism (1)				
P37142	Bifunctional aspartokinase/homoserine dehydrogenase		3.971	0.037
Carbohydrate and energy metabolism (1)				
T2C622	NAD-dependent glyceraldehyde-3-phosphate dehydrogenase (Fragment)	gapC	2.031	0.018
Material Transport (6)				
O04157	Ras-related protein RABG3b	RABG3B	2.464	0.048
O23657	Ras-related protein RABC1	RABC1	2.262	0.037
O49841	Ras-related protein RABC2a	RABC2A	2.047	0.043
Q9LXC0	Guanosine nucleotide diphosphate dissociation inhibitor	At5g09550	2.118	0.016
Q39258	V-type proton ATPase subunit E1	VHA-E1	1.508	0.007
Q9XGM1	V-type proton ATPase subunit D	VHA-D	1.861	0.012
Antioxidant defense (2)				
A0A6C0W0P0	Cysteine proteinase inhibitor	REF2	1.666	0.021
P93836	4-hydroxyphenylpyruvate dioxygenase	HPD	1.687	0.019
Other (4)				
O82803	Small rubber particle protein	SRPP	2.496	0.044
P15252	Rubber elongation factor protein		2.180	0.024
A0A1C9V3S0	NAD(P)-bd_dom domain-containing protein		1.655	0.008
A0A1C9V3Q9	Uncharacterized protein		1.774	0.014

Table 6
Down-regulated DEPs of R-1200_vs_R-600 group.

Accession number	Protein Name	Gene Name	R-1200/R-600 (FC)	*p* value
Signal transduction (1)				
A9TF79	Serine/threonine-protein kinase SRK2A	SRK2A	0.643	0.003
Nucleic acid metabolism (1)				
Q99285	Histone H2B (Fragments)	HIS2B	0.448	0.008
Protein metabolism (10)				
O23627	Glycine–tRNA ligase, mitochondrial 1	At1g29880	0.291	0.044
P49627	60S ribosomal protein L13	RPL13	0.413	0.021
Q9FDZ9	60S ribosomal protein L21-2	RPL21E	0.289	0.001
P45633	60S ribosomal protein L10	RPL10	0.656	0.001
P29345	40S ribosomal protein S6 (Fragment)	RPS6	0.516	0.025
O81361	40S ribosomal protein S8	RPS8	0.511	0.035
P46293	40S ribosomal protein S16	RPS16	0.467	0.049
Q9T029	40S ribosomal protein S25-4	RPS25E	0.289	0.044
A5X2V2	Ribosomal protein L23a (Fragment)		0.402	0.001
P22954	Heat shock 70 kDa protein 2	HSP70-2	0.030	0.001
Carbohydrate and energy metabolism (2)				
Q9C5J7	ATP-dependent 6-phosphofructokinase 7	PFK7	0.322	0.011
Q0V7W6	Alcohol dehydrogenase-like 5	At4g22110	0.057	0.014
Material Transport (2)				
Q08436	Plasma membrane ATPase 3	PMA3	0.509	0.032
M9YX97	TIP-like aquaporin	AQP1	0.214	0.049
Cell wall and cytoskeleton (1)				
Q6VAF9	Tubulin alpha-4 chain		0.638	0.020
Antioxidant defense (1)				
Q6Z6S1	Apoptosis inhibitor 5-like protein API5	API5	0.561	0.030
Secondary metabolism (5)				
P21357	Phospho-2-dehydro-3-deoxyheptonate aldolase 1	SHKA	0.026	0.001
P50303	S-adenosylmethionine synthase 3	SAM3	0.219	0.006
A9NYY0	S-adenosylmethionine synthase 2	METK2	0.270	0.011
Q9LQ04	Bifunctional dTDP-4-dehydrorhamnose 3,5-epimerase/dTDP-4-dehydrorhamnose reductase	NRS/ER	0.233	0.033
A0A6C0VZT6	REF1	REF1	0.644	0.035
Other (1)				
A0A0B5EH65	Photosystem I P700 chlorophyll a apoprotein A1	psaA	0.447	0.037

4.6. Calcium stress may regulate secondary metabolism in D. roosii rhizome cells

Our proteomics results indicated that P2D3DA1, 3PS1CT2, ADD2 were increased by 600 mmol L^{-1} Ca^{2+}, and 3PS1CT2 was also increased by 1200 mmol L^{-1} Ca^{2+} (Tables 1 and 3). These enzymes catalyze the biosynthesis of chorismate, which promotes phenylalanine biosynthesis [68,69]. Phenylalanine is origin of phenylpropanoids biosynthesis [70]. Phenylpropanoids play important role in scavenging ROS induced by abiotic stress [71]. PAL, C4H and 4CL catalyze the first three steps reactions of the phenylpropanoid pathway, lignin biosynthesis and flavonoid biosynthesis are two major pathways of which [70]. In this study, we found that C4H was increased by 600 and 1200 mmol L^{-1} Ca^{2+}, and PAL was increased by 1200 mmol L^{-1} Ca^{2+} (Tables 1 and 3). Our proteomics results revealed that SAMA3 was increased by 600 mmol L^{-1} Ca^{2+} (Table 1). SAMA3 associates with a methyltransferase involved in lignin biosynthesis [72]. Lignin helps plants to cope with various stresses by deposition facilitate cell wall thickening [69]. Thus, calcium stress may regulate lignin synthesis in *D. roosii* rhizome cells. Meanwhile, DHF4R was increased by 600 mmol L^{-1} Ca^{2+} (Table 1). DHF4R could promote the synthesis of anthocyanin [73,74]. Flavonoids have been reported function in scavenging ROS [75,76]. So anthocyanin synthesis in *D. roosii* rhizome cells may also be regulated by calcium stress.

5. Conclusion

In conclusion, the current study revealed various characteristics of physiological indexes and proteins in *D. roosii* rhizome that under calcium stress. Physiological results showed that the *D. roosii* rhizome may subject to osmotic stress after calcium stress treatment. And osmotic stress may result in oxidative damage of rhizome cells. Then rhizome cells may scavenge ROS by synthesizing antioxidant enzymes. Meanwhile, proteomic results showed that calcium stress may affect signal transduction, protein translation, material transport, antioxidant defense and secondary metabolism in *D. roosii* rhizome cells. In addition, our metabolomics results showed that calcium stress affects the amino acid metabolism, flavonoids biosynthesis, lignin biosynthesis, fatty acid metabolism, and other metabolic pathway of *D. roosii* rhizome cells [77]. However, the actual mechanism of adaptation to calcium stress of *D. roosii* rhizome is still unclear. Therefore, further investigation might be necessary to decipher this mechanism by gene analysis. The precise role of stress genes should be validated by using modern biotechnological approaches, and these genes can be useful resources for the development of stress-tolerant plant varieties in future studies.

Funding statement

Dr. Longyan Tan was supported by the National Natural Science Foundation of China (Grant No. 31860056).

Data availability statement

The authors do not have permission to share data.

CRediT authorship contribution statement

Yilin Wu: Writing – original draft, Resources, Methodology, Investigation, Formal analysis, Data curation, Conceptualization. **Hui Li:** Writing – original draft, Resources, Methodology, Investigation, Formal analysis, Data curation. **Shanshan Ma:** Resources, Investigation. **Hongna Ma:** Resources. **Longyan Tan:** Writing – review & editing, Writing – original draft, Validation, Supervision, Resources, Project administration, Funding acquisition, Formal analysis, Data curation, Conceptualization.

Declaration of competing interest

The authors declare that they have no known competing financial interests or personal relationships that could have appeared to influence the work reported in this paper.

Appendix A. Supplementary data

Supplementary data to this article can be found online at https://doi.org/10.1016/j.heliyon.2024.e38260.

References

[1] Z. Jiang, Y. Lian, X. Qin, Rocky desertification in southwest China: impacts, causes, and restoration, Earth Sci. Rev. 132 (2014) 1–12, https://doi.org/10.1016/j.earscirev.2014.01.005.
[2] X. Wei, X. Deng, W. Xiang, P. Lei, S. Ouyang, H. Wen, L. Chen, Calcium content and high calcium adaptation of plants in karst areas of southwestern Hunan, Biogeosciences 15 (2018) 2991–3002, https://doi.org/10.5194/bg-15-2991-2018.
[3] J.H.F. Bothwell, C.K.Y. Ng, The evolution of Ca^{2+} signalling in photosynthetic eukaryotes, New Phytol. 166 (2005) 21–38, https://doi.org/10.1111/j.1469-8137.2004.01312.x.
[4] P.K. Hepler, Calcium: a central regulator of plant growth and development, Plant Cell 8 (2005) 2142–2155, https://doi.org/10.1105/tpc.105.032508.

[5] S.K. Upadhyay, Calcium Transport Elements in Plants, Academic Press, United Kingdom, London, 2021.
[6] K. Guo, C.C. Liu, M. Dong, Ecological adaptation of plants and control of rocky-desertification on karst region of southwest China, Chin. J. Plant Ecol. 35 (2011) 991–999, https://doi.org/10.3724/SP.J.1258.2011.00991.
[7] C.H. Borer, M.N. Hamby, L.H. Hutchinson, Plant tolerance of a high calcium environment via foliar partitioning and sequestration, J. Arid Environ. 85 (2012) 128–131, https://doi.org/10.1016/j.jaridenv.2012.06.004.
[8] S.K. Upadhyay, Calcium channels, OST1 and stomatal defence: current status and beyond, Cells 12 (2023) 127, https://doi.org/10.3390/cells12010127.
[9] S.K. Upadhyay, CPK12 and Ca^{2+}-mediated hypoxia signaling, Plant Signal. Behav. 18 (2023) e2273593, https://doi.org/10.1080/15592324.2023.2273593.
[10] L. Ni, D. Gu, W. He, Y. Huang, Z. Chen, Research advances in plant ecological adaptability in karst area, Chinese, J. Ecol. 38 (2019) 2210–2217.
[11] E. Carafoli, L. Santella, D. Branca, M. Brini, Generation, control, and processing of cellular calcium signals, Crit. Rev. Biochem. Mol. 36 (2001) 107–260, https://doi.org/10.1080/20014091074183.
[12] H.W. Jarrett, C.J. Brown, C.C. Black, M.J. Cormier, Evidence that calmodulin is in the chloroplast of peas and serves a regulatory role in photosynthesis, J. Biol. Chem. 257 (1982) 13795–13804, https://doi.org/10.1016/S0021-9258(18)33519-1.
[13] X. Zhang, L. Liu, J. Gong, J. Tang, M. Tang, Y. Yi, Comparison of calcium distributions leaf cells of *Carpinus pubescens* and *Camellia oleifera* under drought and calcium stress, Pak. J. Bot. 49 (2017) 2139–2143.
[14] O. Fiehn, Combining genomics, metabolome analysis, and biochemical modelling to understand metabolic networks, Comp. Funct. Genom. 2 (2001) 155–168, https://doi.org/10.1002/cfg.82.
[15] O. Fiehn, J. Kopka, P. Dörmann, T. Altmann, R.N. Trethewey, L. Willmitzer, Metabolite profiling for plant functional genomics, Nat. Biotechnol. 18 (2000) 1157–1161, https://doi.org/10.1038/81137.
[16] X. Zhang, Z. Yao, Lycophytes and Ferns of Maolan, Science Press, Beijing, 2017. China.
[17] Y. Wu, H. Ma, S. Ma, W. Li, L. Tan, Physiological, proteomic and metabolomic analysis provide insights into Ca^{2+} tolerance in *Drynaria roosii* leaves, Plant Stress 7 (2023) 100132, https://doi.org/10.1016/j.stress.2023.100132.
[18] J.R. Wiśniewski, A. Zougman, N. Nagaraj, M. Mann, Universal sample preparation method for proteome analysis, Nat. Methods 6 (2009) 359–362, https://doi.org/10.1038/nmeth.1322.
[19] J.R. Wiśniewski, A. Zougman, M. Mann, Combination of FASP and stagetip-based fractionation allows in-depth analysis of the hippocampal membrane proteome, J. Proteome Res. 8 (2009) 5674–5678, https://doi.org/10.1021/pr900748n.
[20] L. Huang, Y. Wu, Y. Wu, L. Tan, Effects of Ca^{2+} with different concentrations on seed germination of *Sophora tonkinensis*, Seed 40 (2021) 81–84, https://doi.org/10.16590/j.cnki.1001-4705.2021.04.081, 89.
[21] H. Ma, D. Xu, L. Tan, Effects of calcium ions stress on roots of *Coix lachryma-jobi* seedling, Lishizhen Med. Mater. Med. Res. 32 (2021) 2746–2748.
[22] L. Tan, Y. He, Effects of calcium ions stress on young leaves of *Fagopyrum dibotrys*, Mod. Agric. Sci. Tech. (2020) 10–12.
[23] Z. Yin, H. Zhang, Q. Zhao, M.J. Yoo, N. Zhu, J. Yu, S. Guo, Y. Miao, S. Chen, Z. Qin, S. Dai, Physiological and comparative proteomic analyses of saline-alkali $NaHCO_3$-responses in leaves of halophyte *Puccinellia tenuiflora*, Plant Soil 437 (2019) 137–158, https://doi.org/10.1007/s11104-019-03955-9.
[24] J. Yu, S. Chen, T. Wang, G. Sun, S. Dai, Comparative proteomic analysis of *Puccinellia tenuiflora* leaves under Na_2CO_3 stress, Int. J. Mol. Sci. 14 (2013) 1740–1762, https://doi.org/10.3390/ijms14011740.
[25] Y. Zhang, Y. Zhang, J. Yu, H. Zhang, L. Wang, S. Wang, S. Guo, Y. Miao, S. Chen, Y. Li, S. Dai, NaCl-responsive ROS scavenging and energy supply in alkaligrass callus revealed from proteomic analysis, BMC Genom. 20 (2019) 990, https://doi.org/10.1186/s12864-019-6325-6.
[26] S. Tyagi Shumayla, Y. Sharma, Madhu, A. Sharma, A. Pandey, K. Singh, S.K. Upadhyay, Expression of *TaNCL2-A* ameliorates cadmium toxicity by increasing calcium and enzymatic antioxidants activities in *Arabidopsis*, Chemosphere 329 (2023) 138636, https://doi.org/10.1016/j.chemosphere.2023.138636.
[27] M. Zhang, S. Zhang, Mitogen-activated protein kinase cascades in plant signaling, J. Integr. Plant Biol. 64 (2022) 301–341, https://doi.org/10.1111/jipb.13215.
[28] T. Mizoguchi, K. Ichimura, K. Shinozaki, Environmental stress response in plants: the role of mitogen-activated protein kinases, Trends Biotechnol. 15 (1997) 15–19, https://doi.org/10.1016/S0167-7799(96)10074-3.
[29] K. Kumar, A.K. Sinha, Overexpression of constitutively active mitogen activated protein kinase kinase 6 enhances tolerance to salt stress in rice, Rice 6 (2013) 25, https://doi.org/10.1186/1939-8433-6-25.
[30] A. Aitken, 14-3-3 proteins: a historic overview, Semin. Cancer Biol. 16 (2006) 162–172, https://doi.org/10.1016/j.semcancer.2006.03.005.
[31] M. Ormancey, P. Thuleau, C. Mazars, V. Cotelle, CDPKs and 14-3-3 proteins: emerging duo in signaling, Trends Plant Sci. 22 (2017) 263–272, https://doi.org/10.1016/j.tplants.2016.11.007.
[32] S.L. Ho, L.F. Huang, C.A. Lu, S.L. He, C.C. Wang, S.P. Yu, J. Chen, S.M. Yu, Sugar starvation- and GA-inducible calcium-dependent protein kinase 1 feedback regulates GA biosynthesis and activates a 14-3-3 protein to confer drought tolerance in rice seedlings, Plant Mol. Biol. 81 (2013) 347–361, https://doi.org/10.1007/s11103-012-0006-z.
[33] C.L. Guo, Q. Chen, X.L. Zhao, X.Q. Chen, Y. Zhao, L. Wang, K.Z. Li, Y.X. Yu, L.M. Chen, Al-enhanced expression and interaction of 14-3-3 protein and plasma membrane H^+-ATPase is related to Al-induced citrate secretion in an Al-resistant black soybean, Plant Mol. Biol. Rep. 31 (2013) 1012–1024, https://doi.org/10.1007/s11105-013-0569-0.
[34] S. Merlot, N. Leonhardt, F. Fenzi, C. Valon, M. Costa, L. Piette, e. al, Constitutive activation of a plasma membrane H^+-ATPase prevents abscisic acid-mediated stomatal closure, EMBO J. 26 (2007) 3216–3226, https://doi.org/10.1038/sj.emboj.7601750.
[35] C. Dai, Y. Lee, I.C. Lee, H.G. Nam, J.M. Kwak, Calmodulin 1 regulates senescence and ABA response in Arabidopsis, Front. Plant Sci. 9 (2018) 803, https://doi.org/10.3389/fpls.2018.00803.
[36] W. Tang, T. Kim, J.A. Oses-Prieto, Y. Sun, Z. Deng, S. Zhu, R. Wang, A.L. Burlingame, Z. Wang, BSKs mediate signal transduction from the receptor kinase BRI1 in *Arabidopsis*, Science 321 (2008) 557–560, https://doi.org/10.1126/science.1156973.
[37] W. Tang, M. Yuan, R. Wang, Y. Yang, C. Wang, J.A. Oses-Prieto, T. Kim, H. Zhou, Z. Deng, S.S. Gampala, J.M. Gendron, E.M. Jonassen, C. Lillo, A. DeLong, A. L. Burlingame, Y. Sun, Z. Wang, PP2A activates brassinosteroid-responsive gene expression and plant growth by dephosphorylating BZR1, Nat. Cell Biol. 13 (2011) 124–131, https://doi.org/10.1038/ncb2151.
[38] D. Bartels, R. Sunkar, Drought and salt tolerance in plants, Crit. Rev. Plant Sci. 24 (2005) 23–58, https://doi.org/10.1080/07352680590910410.
[39] R. Mittler, S.I. Zandalinas, Y. Fichman, F.V. Breusegem, Reactive oxygen species signalling in plant stress responses, Nat. Rev. Mol. Cell Biol. 23 (2022) 663–679, https://doi.org/10.1038/s41580-022-00499-2.
[40] Y. Sharma, Shumayla Ishu, S. Dixit, K. Singh, S.K. Upadhyay, Decoding the features and potential roles of respiratory burst oxidase homologs in bread wheat, Curr. Plant Biol. 37 (2024) 100315, https://doi.org/10.1016/j.cpb.2023.100315.
[41] J. de la Cruz, K. Karbstein, J.L. Woolford, Functions of ribosomal proteins in assembly of eukaryotic ribosomes in vivo, Annu. Rev. Biochem. 84 (2015) 93–129, https://doi.org/10.1146/annurev-biochem-060614-033917.
[42] S. Baindur-Hudson, A.L. Edkins, G.L. Blatch, Hsp70/Hsp90 organising protein (hop): beyond interactions with chaperones and prion proteins, in: G.L. Blatch, A. L. Edkins (Eds.), The Networking of Chaperones by Co-chaperones. Subcellular Biochemistry, vol. 78, Springer, Cham, 2015.
[43] L.G.J. Nijtmans, L.d. Jong, M.A. Sanz, P.J. Coates, J.A. Berden, J.W. Back, A.O. Muijsers, H.v. d. Spek, L.A. Grivell, Prohibitins act as a membrane-bound chaperone for the stabilization of mitochondrial proteins, EMBO J. 19 (2000) 2444–2451, https://doi.org/10.1093/emboj/19.11.2444.
[44] S.H. Kim, S.J. Roux, An *Arabidopsis* ran-binding protein, AtRanBP1c, is a co-activator of ran GTPase-activating protein and requires the C-terminus for its cytoplasmic localization, Planta 216 (2003) 1047–1052, https://doi.org/10.1007/s00425-002-0959-2.
[45] K. Li, C. Xu, K. Zhang, A. Yang, J. Zhang, Proteomic analysis of roots growth and metabolic changes under phosphorus deficit in maize (*Zea mays* L.) plants, Proteomics 7 (2007) 1501–1512, https://doi.org/10.1002/pmic.200600960.
[46] G. Batelli, P.E. Verslues, F. Agius, Q. Qiu, H. Fujii, S. Pan, et al., SOS2 promotes salt tolerance in part by interacting with the vacuolar H^+-ATPase and upregulating its transport activity, Mol. Cell Biol. 27 (2007) 7781–7790, https://doi.org/10.1128/MCB.00430-07.
[47] H. Damke, T. Baba, D.E. Warnock, S.L. Schmid, Induction of mutant dynamin specifically blocks endocytic coated vesicle formation, J. Cell Biol. 127 (1994) 915–934, https://doi.org/10.1083/jcb.127.4.915.

[48] C. Spitzer, F.C. Reyes, R. Buono, M.K. Sliwinski, T.J. Haas, M.S. Otegui, The ESCRT-Related CHMP1 A and B proteins mediate multivesicular body sorting of auxin carriers in *Arabidopsis* and are required for plant development, Plant Cell 21 (2009) 749–766, https://doi.org/10.1105/tpc.108.064865.
[49] S. Kakuta, J. Yamaguchi, C. Suzuki, M. Sasaki, S. Kazuno, Y. Uchiyama, Small GTPase rab1b is associated with ATG9A vesicles and regulates autophagosome formation, FASEB J 31 (2017) 3757–3773, https://doi.org/10.1096/fj.201601052R.
[50] H. Plutner, A.D. Cox, S. Pind, R. Khosravi-Far, J.R. Bourne, R. Schwaninger, C.J. Der, W.E. Balch, Rab1b regulates vesicular transport between the endoplasmic reticulum and successive golgi compartments, J. Cell Biol. 115 (1991) 31–43, https://doi.org/10.1083/jcb.115.1.31.
[51] S.I. Kwon, H.J. Cho, J.H. Jung, K. Yoshimoto, K. Shirasu, O.K. Park, The rab GTPase RabG3b functions in autophagy and contributes to tracheary element differentiation in *Arabidopsis*, Plant J. 64 (2010) 151–164, https://doi.org/10.1111/j.1365-313X.2010.04315.x.
[52] S.I. Kwon, H.J. Cho, S.R. Kim, O.K. Park, The rab GTPase RabG3b positively regulates autophagy and immunity-associated hypersensitive cell death in *Arabidopsis*, Plant Physiol. 161 (2013) 1722–1736, https://doi.org/10.1104/pp.112.208108.
[53] J. Peng, H. Ilarslan, E.S. Wurtele, D.C. Bassham, 5AtRabD2b and AtRabD2c have overlapping functions in pollen development and pollen tube growth, BMC Plant Biol. 11 (2011) 25, https://doi.org/10.1186/1471-2229-11-25.
[54] X. Fang, Analyze the Effect of MeJA on Autophagy in Laticifers of *Euphorbia Kansui* Liou Based on the iTRAQ Proteomics Technique, Northwest University, 2020.
[55] F. Barrieu, F. Chaumont, M.J. Chrispeels, High expression of the tonoplast aquaporin *ZmTIP1* in epidermal and conducting tissues of maize, Plant Physiol. 117 (1998) 1153–1163, https://doi.org/10.1104/pp.117.4.1153.
[56] C. Maurel, Aquaporins and water permeability of plant membranes, Annu. Rev. Plant Physiol. Plant Mol. Biol. 48 (1997) 399–429, https://doi.org/10.1146/annurev.arplant.48.1.399.
[57] X. Sarda, D. Tousch, K. Ferrare, E. Legrand, J.M. Dupuis, F. Casse-Delbart, T. Lamaze, Two TIP-like genes encoding aquaporins are expressed in sunflower guard cells, Plant J. 12 (1997) 1103–1111, https://doi.org/10.1046/j.1365-313X.1997.12051103.x.
[58] M. Heckwolf, D. Pater, D.T. Hanson, R. Kaldenhoff, The *Arabidopsis thaliana* aquaporin AtPIP1;2 is a physiologically relevant CO_2 transport facilitator, Plant J. 67 (2011) 795–804, https://doi.org/10.1111/j.1365-313X.2011.04634.x.
[59] I.C. Mori, J. Rhee, M. Shibasaka, S. Sasano, T. Kaneko, T. Horie, M. Katsuhara, CO_2 transport by PIP2 aquaporins of barley, Plant Cell Physiol. 55 (2014) 251–257, https://doi.org/10.1093/pcp/pcu003.
[60] Madhu, A. Kaur, K. Singh, S.K. Upadhyay, Ascorbate oxidases in bread wheat: gene regulatory network, transcripts profiling, and interaction analyses provide insight into their role in plant development and stress response, Plant Growth Regul. 103 (2024) 209–224, https://doi.org/10.1007/s10725-023-01103-z.
[61] A. Sharma Madhu, A. Kaur, K. Singh, S.K. Upadhyay, Modulation in gene expression and enzyme activity suggested the roles of monodehydroascorbate reductase in development and stress response in bread wheat, Plant Sci. 338 (2024) 111902, https://doi.org/10.1016/j.plantsci.2023.111902.
[62] V.D. Rajput, Harish, R.K. Singh, K.K. Verma, L. Sharma, F.R. Quiroz-Figueroa, M. Meena, V.S. Gour, T. Minkina, S. Sushkova, S. Mandzhieva, Recent developments in enzymatic antioxidant defence mechanism in plants with special reference to abiotic stress, Biology 10 (2021) 267, https://doi.org/10.3390/biology10040267.
[63] X. Cheng, G. Deng, Y. Su, J.J. Liu, Y. Yang, G.H. Du, Z.Y. Chen, F.H. Liu, Protein mechanisms in response to NaCl-stress of salt-tolerant and salt-sensitive industrial hemp based on iTRAQ technology, Ind. Crop. Prod. 83 (2016) 444–452, https://doi.org/10.1016/j.indcrop.2015.12.086.
[64] A. Grover, Plant chitinases: genetic diversity and physiological roles, Crit. Rev. Plant Sci. 31 (2012) 57–73, https://doi.org/10.1080/07352689.2011.616043.
[65] Z.D. Xu, R.L. Jing, Q. Gan, H.P. Zeng, X.H. Sun, H. Leung, T. Lu, G. Liu, Drought-tolerant gene screening in wheat using rice microarray, Chinese J, Agric. Biotechnol. 5 (2008) 43–48, https://doi.org/10.1017/S1479236207001969.
[66] B.A. Pandian, R. Sathishraj, M. Djanaguiraman, P.V.V. Prasad, M. Jugulam, Role of cytochrome P450 Enzymes in plant stress response, Antioxidants 9 (2020) 454, https://doi.org/10.3390/antiox9050454.
[67] S. Lorrain, B. Lin, M.C. Auriac, T. Kroj, P. Saindrenan, M. Nicole, C. Balaguee, D. Roby, VASCULAR ASSOCIATED DEATH1, a novel gram domain–containing protein, is a regulator of cell death and defense responses in vascular tissues, Plant Cell 16 (2004) 2217–2232, https://doi.org/10.1105/tpc.104.022038.
[68] H.K. Hund, B. Keller, F. Lingens, Phenylalanine and tyrosine biosynthesis in sporeforming members of the order actinomycetales, Z. Naturforsch C. 42 (1987) 387–393, https://doi.org/10.1515/znc-1987-0410.
[69] C. Lemaître, P. Bidet, J.F. Benoist, D. Schlemmer, E. Sobral, C. d"Humières, S. Bonacorsi, The *ssbL* gene harbored by the col V plasmid of an *Escherichia coli* neonatal meningitis strain is an auxiliary virulence factor boosting the production of siderophores through the shikimate pathway, J. Bacteriol. 196 (2014) 1343–1349, https://doi.org/10.1128/JB.01153-13.
[70] N.Q. Dong, H.X. Lin, Contribution of phenylpropanoid metabolism to plant development and plant–environment interactions, J. Integr. Plant Biol. 63 (2021) 180–209, https://doi.org/10.1111/jipb.13054.
[71] A. Fini, L. Guidi, F. Ferrini, C. Brunetti, M.D. Ferdinando, S. Biricolti, e. al, Drought stress has contrasting effects on antioxidant enzymes activity and phenylpropanoid biosynthesis in *Fraxinus ornus* leaves: an excess light stress affair? J. Plant Physiol. 169 (2012) 929–939, https://doi.org/10.1016/j.jplph.2012.02.014.
[72] B. Shen, C. Li, M.C. Tarczynski, High free-methionine and decreased lignin content result from a mutation in the *Arabidopsis* S-adenosyl-L-methionine synthetase 3 gene, Plant J. 29 (2002) 371–380, https://doi.org/10.1046/j.1365-313X.2002.01221.x.
[73] B.W. Shirley, S. Hanley, H.M. Goodman, Effects of ionizing radiation on a plant genome: analysis of two *Arabidopsis* transparent testa mutation, Plant Cell 4 (1992) 333–347, https://doi.org/10.1105/tpc.4.3.333.
[74] B. Winkel-Shirley, Flavonoid biosynthesis. a colorful model for genetics, biochemistry, cell biology, and biotechnolog, Plant Physiol. 126 (2001) 485–493, https://doi.org/10.1104/pp.126.2.485.
[75] N. Jiang, A.I. Doseff, E. Grotewold, Flavones: from biosynthesis to health benefits, Plants 5 (2016) 27, https://doi.org/10.3390/plants5020027.
[76] R. Nakabayashi, K. Yonekura-Sakakibara, K. Urano, M. Suzuki, Y. Yamada, T. Nishizawa, F. Matsuda, M. Kojima, H. Sakakibara, K. Shinozaki, A.J. Michael, T. Tohge, M. Yamazaki, K. Saito, Enhancement of oxidative and drought tolerance in *Arabidopsis* by overaccumulation of antioxidant flavonoids, Plant J. 77 (2014) 367–379, https://doi.org/10.1111/tpj.12388.
[77] Y. Wu, H. Li, H. Ma, W. Li, L. Tan, Analysis of differentially expressed metabolites in *Drynaria roosii* rhizome in response to calcium stress, Guihaia 44 (2024) 531–540, https://doi.org/10.11931/guihaia.gxzw202302017.